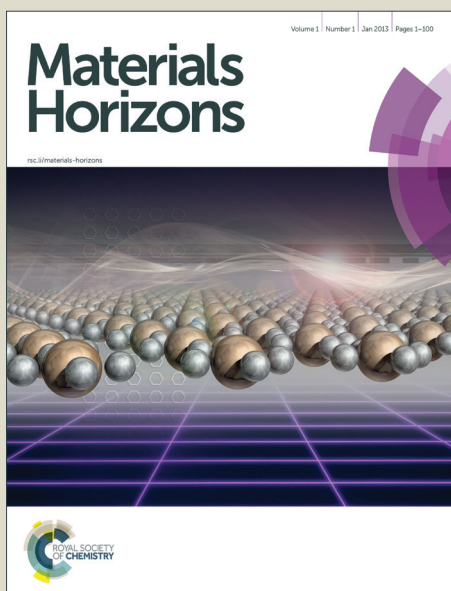


Materials Horizons

Accepted Manuscript



This is an *Accepted Manuscript*, which has been through the Royal Society of Chemistry peer review process and has been accepted for publication.

Accepted Manuscripts are published online shortly after acceptance, before technical editing, formatting and proof reading. Using this free service, authors can make their results available to the community, in citable form, before we publish the edited article. We will replace this *Accepted Manuscript* with the edited and formatted *Advance Article* as soon as it is available.

You can find more information about *Accepted Manuscripts* in the [Information for Authors](#).

Please note that technical editing may introduce minor changes to the text and/or graphics, which may alter content. The journal's standard [Terms & Conditions](#) and the [Ethical guidelines](#) still apply. In no event shall the Royal Society of Chemistry be held responsible for any errors or omissions in this *Accepted Manuscript* or any consequences arising from the use of any information it contains.

Conceptual Insights

The importance of molecular semiconductors in emerging information and display technologies is progressively increasing. A key element of bringing these technologies to the next level is an improved control over charge carrier, i.e., polaron, properties. The nature of these polarons, excess charges strongly coupled to structural degrees of freedom, must be fully understood to achieve this control. The traditional picture of polarons established in the organic electronics community has not been critically questioned since the early 1980's, despite the fact that the photoelectron spectra obtained on molecular semiconductors comprising polarons were frequently at odds with this model. We now show that this traditional model, which predicts singly occupied molecular levels within the energy gap of the semiconductor, needs to be revised. For molecular ions, the respective frontier molecular level is split by strong on-site Coulomb repulsion into an upper unoccupied and a lower occupied sub-level, only one of which lies within the semiconductor gap. By including also inter-site Coulomb interaction between molecular ions and surrounding neutral molecules, we provide a complete picture for the photoelectron spectral signature of the energy levels in hole- and electron-doped molecular semiconductors. Our results call for a re-interpretation of many previous reports, and will enable a deeper understanding of charges in these complex systems in the future.

Probing the Energy Levels in Hole-doped Molecular Semiconductors

Stefanie Winkler^{1,2}, Patrick Amsalem¹, Johannes Frisch¹, Martin Oehzelt^{1,2},
Georg Heimel^{‡,1}, and Norbert Koch^{*,1,2}

¹ *Institut für Physik & IRIS Adlershof, Humboldt-Universität zu Berlin, Brook-Taylor-Straße 6,
D-12489 Berlin, Germany*

² *Helmholtz-Zentrum Berlin für Materialien und Energie GmbH, Bereich Erneuerbare
Energien, D-12489 Berlin, Germany*

Abstract

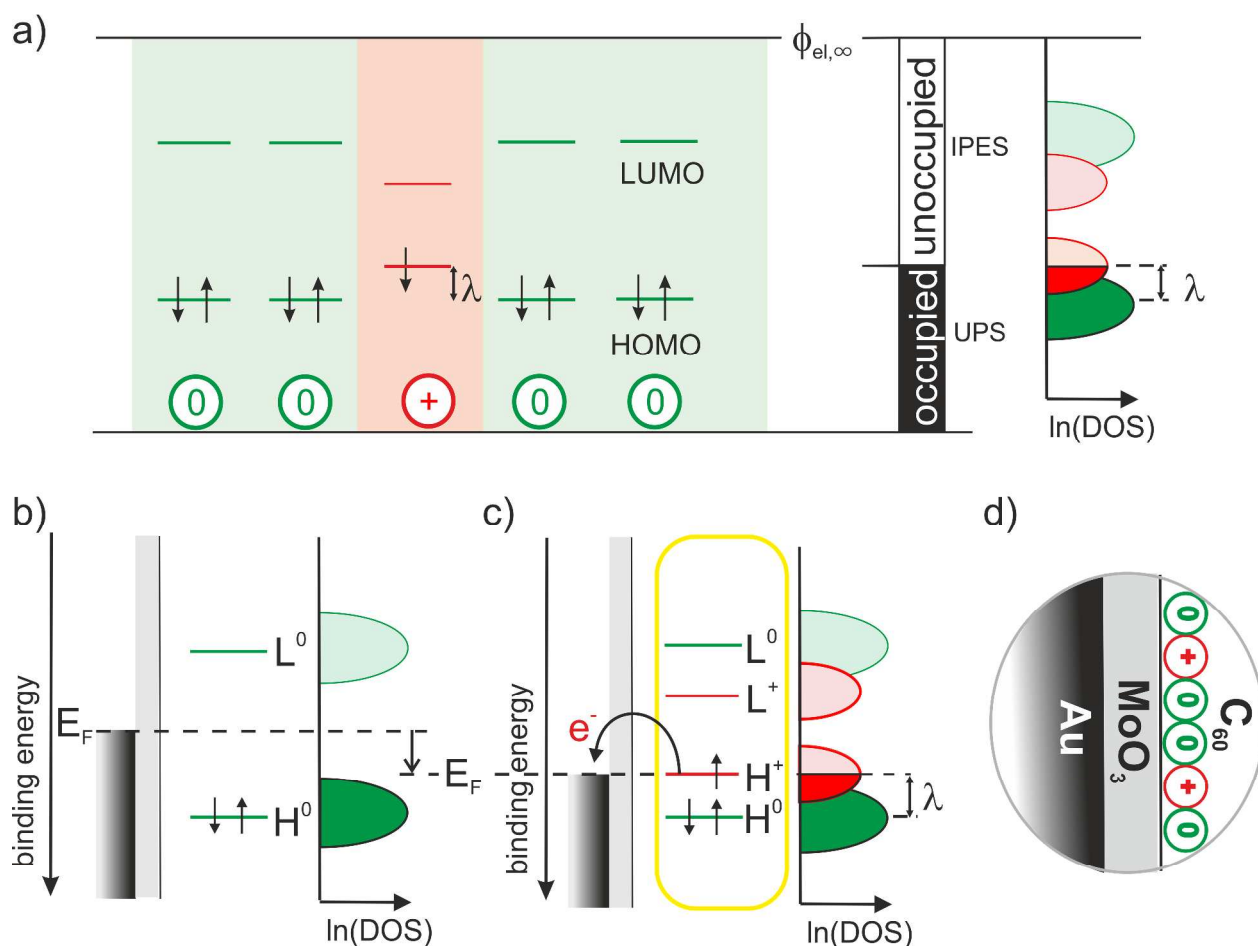
Understanding the nature of polarons – the fundamental charge carriers in molecular semiconductors – is indispensable for rational material design that targets superior (opto-) electronic device functionality. The traditionally conceived picture of the corresponding energy levels invokes singly occupied molecular states within the energy gap of the semiconductor. Here, by employing a combined theoretical and multi-technique experimental approach, we show that this picture needs to be revised. Upon introducing an excess electron or hole into the material, the respective frontier molecular level is split by strong on-site Coulomb repulsion into an upper unoccupied and a lower occupied sub-level, only one of which is located within the semiconductor gap. By including also inter-site Coulomb interaction between molecular ions and circumjacent neutral molecules, we provide a complete picture for the electronic structure of molecular semiconductors in the presence of excess charges. With this understanding, a critical re-examination of previous results is called for, and future investigations of the properties and dynamics of polarons in weakly interacting molecular systems are put on sound footing.

[‡] Email: georg.heimel@physik.hu-berlin.de

^{*} Email: norbert.koch@physik.hu-berlin.de

28 Molecular semiconductors are progressively employed in electronic and optoelectronic devices
29 because of the wide tunability of their optical gap, e.g., in organic light-emitting diodes (OLEDs),
30 their high light absorption cross section, e.g., in organic photovoltaic cells (OPVCs), and also
31 their potential for low-cost large-area processability from solution, e.g., by printing. At the same
32 time, however, the performance of such devices often suffers from the relatively low charge
33 carrier mobility in molecular semiconductors compared to their inorganic counterparts. To
34 address this critical issue, it is of paramount importance to understand in detail the nature of
35 charge carriers (excess electrons and holes) in these materials, where strong coupling of both
36 electrons and holes to (inter- and intra-) molecular vibrations leads to polaron formation¹⁻⁶.

37 For a positively charged molecule, that is, for a cation, in a matrix of neutral molecules, Fig. 1(a)
38 shows the relevant single-particle energy levels and their occupation according to the commonly
39 accepted and widely used picture^{2, 3, 7-14}. Removing an electron from the highest occupied
40 molecular orbital (HOMO) level of a neutral molecule leads to its geometrical relaxation and a
41 concomitant shift by the reorganization energy λ of the now singly occupied state into the energy
42 gap of the semiconductor². Concomitantly with this change of energy levels also the optical
43 transitions of cations change with respect to neutral molecules (usually sub-gap absorption),
44 which, however, are not discussed here.



45

46 Fig. 1 **Traditional view of the molecular single-particle energy levels and how they can be**
 47 **created and measured:** (a) Single-particle energy levels for neutral molecules (green)
 48 surrounding a cation (red) with respect to a common vacuum level $\phi_{el,\infty}$, their experimental
 49 accessibility to (inverse) photoelectron spectroscopy depending on their occupancy and the
 50 resulting density of states (DOS) on a logarithmic scale, $\ln(\text{DOS})$, as proposed according to
 51 common assumptions in Ref.7 (b) Single-particle energy level diagrams for a neutral molecule
 52 on an intermediate and (c) a high work-function substrate causing electron transfer that results
 53 in cations.^{2, 3, 7-10} The latter is realized here with the Au/MoO₃/C₆₀-heterostructure (d).

54

55 Based on this picture, it is widely anticipated^{7, 10, 11} that (i) the doubly occupied states should be
 56 experimentally accessible by ultraviolet photoelectron spectroscopy (UPS), (ii) the empty states
 57 by inverse photoelectron spectroscopy (IPES) and (iii) the singly occupied state by means of *both*
 58 UPS and IPES; these expectations for the density of states (DOS) in the molecular solid are
 59 illustrated in the right panel of Fig. 1 (adapted from Ref. 7). Despite best efforts by means of

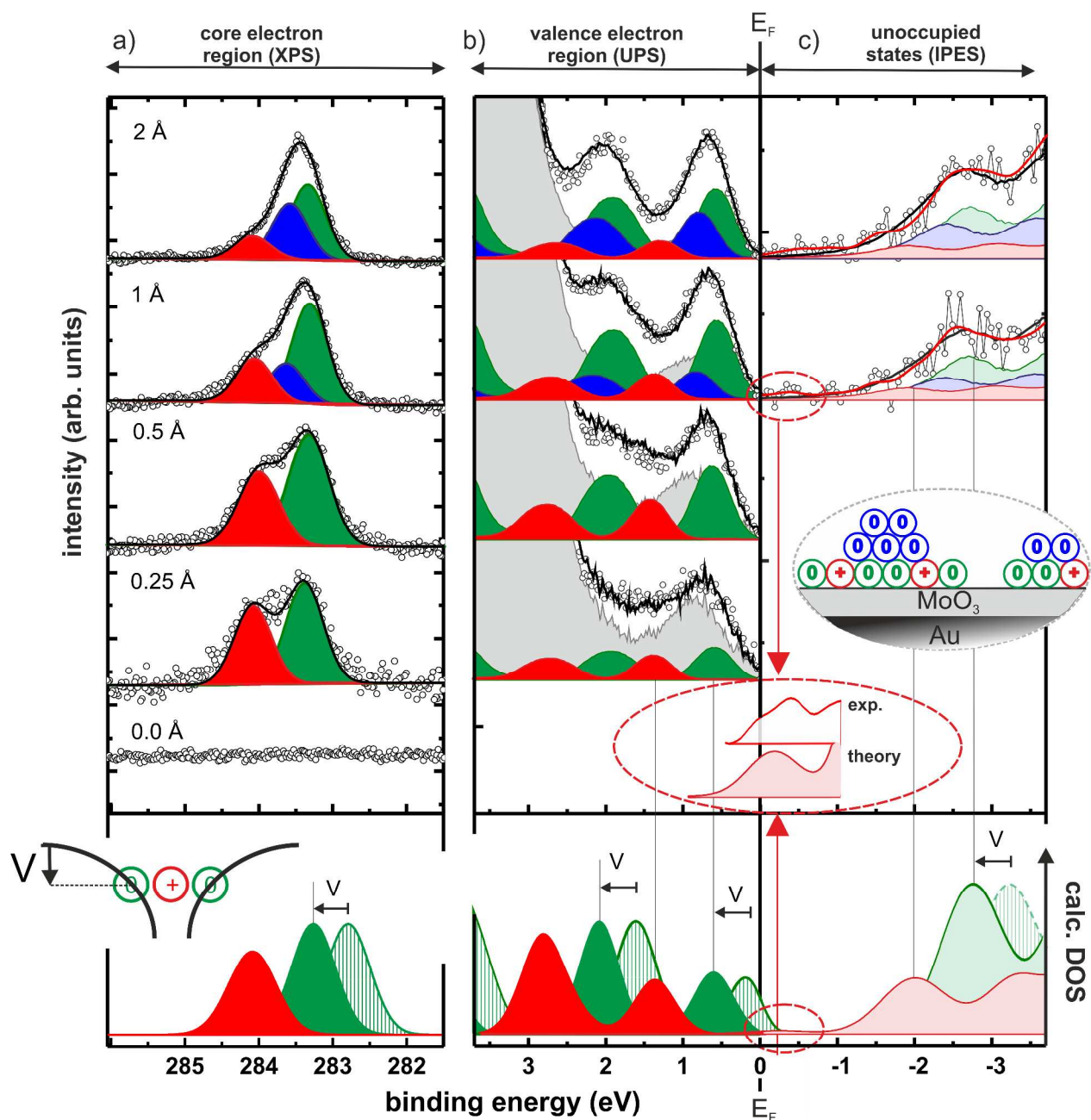
60 UPS^{9, 15}, however, clear spectral evidence for the relaxed cation's HOMO level within the gap is
61 still missing.

62 Here, we seek to provide such evidence and realize that it is challenging even to generate the
63 species of interest, i.e., molecular cations in a matrix of neutral but otherwise identical molecules:
64 When generated by p-doping, the singly occupied state of the cation can hardly be distinguished
65 from the filled lowest unoccupied molecular orbital (LUMO) level of the dopant⁹ and, moreover,
66 strong electronic coupling between molecular HOMO and dopant LUMO cannot generally be
67 excluded^{16, 17}, which might significantly distort the DOS in the relevant energy range. Likewise,
68 electronic coupling to atomically clean metal surfaces is known to not yield integer-charged
69 molecules but to result in pronounced mixing of metal and molecular states instead^{18, 19}.

70 This hybridization with the metal, however, can be inhibited by inserting an insulator between
71 metal and molecules, reminiscent of the situation in a p-type organic field-effect transistor
72 (OFET) under applied (negative) gate voltage²⁰. Simplifying this approach, cations can be
73 generated by employing a metal-supported, ultra-thin dielectric with a work function (WF) higher
74 than the ionization energy (IE) of subsequently deposited molecules as depicted in Fig. 1(b-c).
75 Thereby, the Fermi-level (E_F) of the underlying metal is moved into the occupied DOS of the
76 molecules, causing electron transfer from the molecules across the insulator into the metal to
77 establish electronic equilibrium.

78 In the present study, this was realized with a 1.2 nm thin MoO₃ layer (WF = 6.8 eV) supported by
79 an atomically clean Au(111) single-crystal surface. To facilitate the detection of the potentially
80 low cation concentrations, we employed C₆₀ (IE = 6.4 eV) as hole accumulation layer due to its
81 high orbital degeneracy (HOMO:5, LUMO:3); the full heterostructure is sketched in Fig. 1(d)
82 (see also Methods section).

83 To confirm the presence of C_{60} cations, X-ray photoelectron spectroscopy (XPS) was first used to
84 probe the C1s core-levels, which are known to be at different binding energy for the molecule in
85 its neutral and cationic state²¹. Fig. 2(a) shows the C1s spectra for increasing C_{60} coverage,
86 together with the results of the applied fitting procedure. The bottom curve in the figure shows
87 that no carbon is adsorbed on the pristine MoO_3 . Upon C_{60} deposition, two distinct C1s peaks
88 emerge, which are split by ~ 0.7 eV and evidence the coexistence of cationic (high binding
89 energy - red) and neutral (low binding energy - green) molecules at the interface. This literature-
90 based assignment²¹ is also fully in line with the expectation of a decreasing fraction of charged
91 molecules with increasing coverage in the monolayer regime^{22, 23}, as the cation component
92 becomes weaker compared to the neutral one with increasing coverage. Notably, the fraction of
93 C_{60} cations is in the range of 40% below 1 Å nominal coverage (for other thicknesses see ESI).
94 From 1 Å nominal coverage onwards, a third C1s peak (blue) is required to maintain the quality
95 of the fit. We attribute this additional component to neutral C_{60} molecules in a second layer, as
96 illustrated in the inset of Fig. 2(c). While its presence is of no further consequence for the
97 discussion below, it supports the notion of hole accumulation within the first layer, as it is
98 energetically aligned according to the electrostatics of energy level bending (see ESI).²⁴⁻²⁶



99

100 Fig. 2 Spectra from photoemission and modelling of C_{60} layers comprising neutral molecules
 101 and radical cations: (a) C_{60} -coverage dependent (inverse) photoelectron spectra of (a) C1s core-
 102 levels, (b) occupied, and (c) unoccupied valence states. The experimental curves (black circles)
 103 can be reconstructed by a superposition (black line) of accordingly shifted and scaled thick-film
 104 C_{60} spectra for charged (red), neutral monolayer (green), and multilayer (blue) contributions
 105 with a background of bare $MoO_3/Au(111)$ (grey curve for UPS, see ESI for unoccupied states).
 106 Inset in c) illustrates the C_{60} growth mode. Bottom of b) and c) shows the DFT-calculated DOS of
 107 the neutral (green striped) and positively charged (red) molecules. Both were rigidly shifted in
 108 energy so that the occupied cation features match the experiment. To account for the Coulomb

109 potential well created by nearby cations (inset of bottom panel), the calculated DOS of the
110 neutral molecules is further shifted by $V=0.5$ eV to higher binding energy. The magnification of
111 the region close to E_F highlights experimental and theoretical evidence for an unoccupied
112 HOMO-derived state slightly above E_F .

113

114 Regarding the electrostatics within the hole-accumulating (sub)monolayer itself, it is important to
115 note that, here, the neutral molecules observed in XPS reside within the Coulomb potential well
116 created by nearby cations, as schematically sketched at the bottom of Fig. 2(a). Thereby, all
117 energy levels of these neutral C_{60} molecules are shifted rigidly to higher binding energy (by an
118 amount V). This ensures that their (fully occupied) HOMO levels now come to lie entirely below
119 E_F , thus preventing them from undergoing electron transfer to the underlying metal and,
120 consequently, from becoming cations themselves. This process enables the coexistence of neutral
121 and cationic molecules in the monolayer²³. The magnitude of V can be estimated by comparing
122 the experimentally obtained core-level shift to that calculated by density functional theory (DFT)
123 for a single C_{60} molecule in both its neutral and its charged state (see Methods section). Because
124 calculations performed on single molecules cannot account for the mutual Coulomb interaction
125 present in experiment, comparing the theoretically and experimentally obtained C1s binding
126 energy differences of ~ 1.2 eV and ~ 0.7 eV, respectively, suggest $V \approx 0.5$ eV.

127 Having confirmed the presence of C_{60} cations in the (sub)monolayer, we now turn to UPS to
128 study its valence electronic structure, as shown in Fig. 2(b). With increasing coverage, molecular
129 spectral features arise until, at about 30 \AA (see ESI), the typical thick-film spectrum of neutral C_{60}
130 is obtained^{27, 28}. For $< 1 \text{ \AA}$ coverage, however, subtraction of such a spectrum and the substrate
131 contribution (each suitably scaled) inevitably yields a residual that resembles another C_{60} thick-
132 film spectrum over a wide binding energy range (see ESI). This implies the presence of a second,
133 chemically intact, but energy-shifted C_{60} species as, in fact, expected from XPS. Indeed, the

134 superposition of suitably scaled contributions from the substrate and two energetically shifted C_{60}
135 spectra, one accounting for the neutral molecules and one for the cations, perfectly reconstructs
136 the measured thin-film data, as depicted in Fig. 2(b). This spectral deconvolution is further
137 justified by our DFT results, which confirm that the shape of the DOS is almost identical for
138 neutral and cationic C_{60} , as shown in the bottom of Fig. 2(b) and (c).

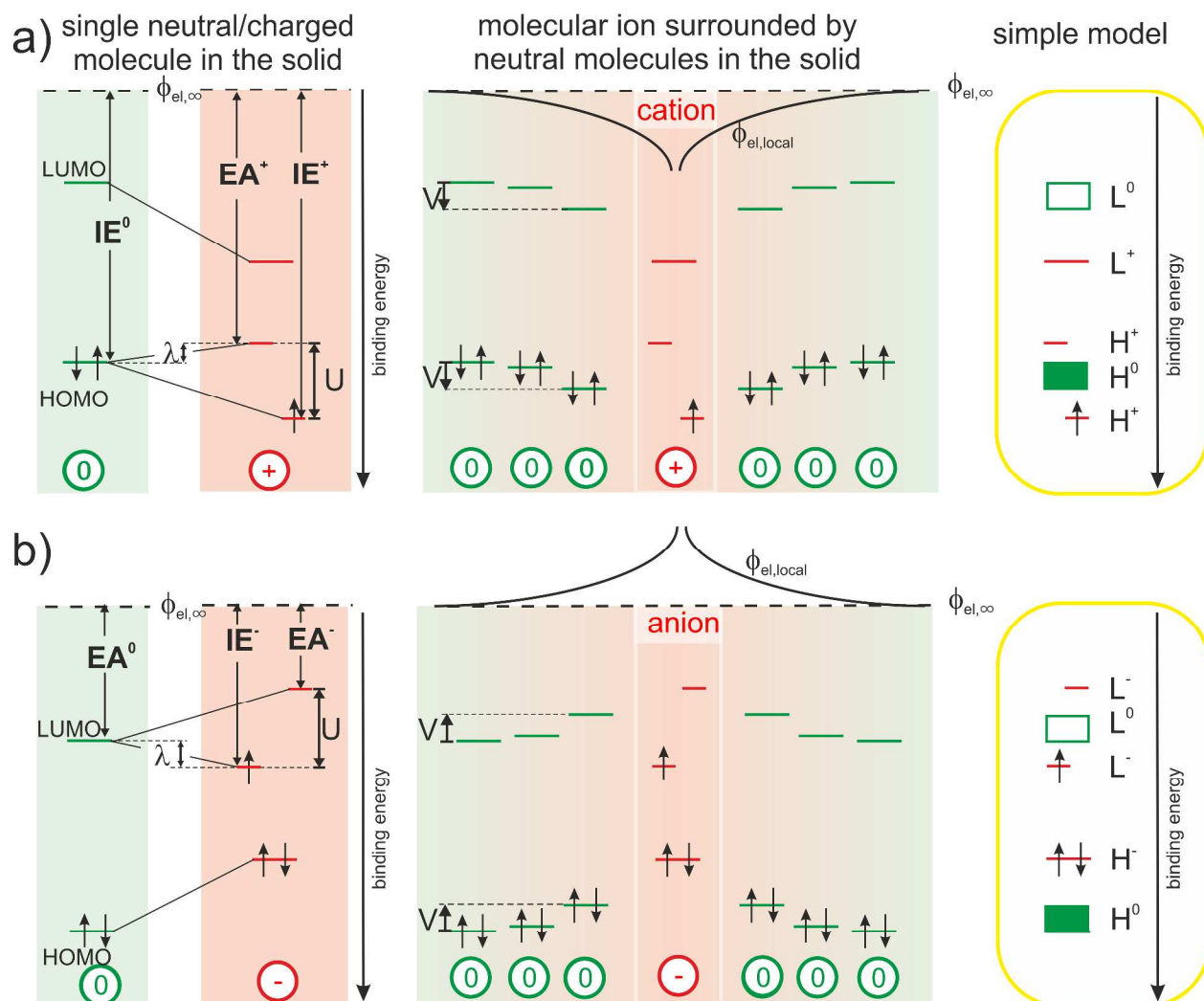
139 Because, as in XPS, the high binding energy spectral contribution decreases with increasing
140 submonolayer coverage, the assignment of these two C_{60} species – also fully supported by DFT –
141 has to be: The *low* binding energy component corresponds to neutral molecules (green) and the
142 component at 0.8 eV *higher* binding energy corresponds to molecular cations (red). This is in
143 clear contrast to the expectations outlined for UPS in Fig. 1(a,c).

144 To assess the validity of these expectations also for the unoccupied states, we applied the
145 complementary spectroscopic technique IPES. The spectral intensity associated with C_{60} was
146 retrieved by subtracting a suitably scaled substrate contribution from the raw data (see ESI). Fig.
147 2(c) shows the obtained difference-spectra for increasing nominal film thickness, starting with a
148 C_{60} coverage of 1 Å; for lower coverages the IPES intensity is insufficient due to the inherently
149 low photon yield of the method. A superposition of three C_{60} contributions (one each for cations
150 in the monolayer, neutral molecules in the monolayer, and neutral molecules in the second layer)
151 with relative weights and energy offsets in accordance with both XPS and UPS satisfactorily
152 reproduces the obtained IPES spectra.

153 More importantly, however, both experiment and theory reveal the presence of an *unoccupied*
154 HOMO-derived state of the cation, attributed to one out of ten electrons missing in the fivefold
155 degenerate HOMO of neutral C_{60} (see ESI for a discussion of the reliability of this assertion and
156 experimental details). This spectral feature is located close to and above E_F (in IPES:

157 -0.25 ± 0.25 eV binding energy) as deduced from the magnified comparison of calculated DOS
158 and experimental spectrum in Fig. 2(c).

159 So, disconcertingly, the IPES results fulfil the expectations outlined in Fig. 1(a,c) while the UPS
160 results are in strong contrast. To elucidate this striking discrepancy, we start out the discussion
161 with Fig. 3(a): The energy required to remove an electron from a neutral molecule in the solid
162 (IE^0) via UPS equals the energy gain upon returning it onto the relaxed cation (EA^+) via IPES
163 plus the reorganization energy λ ^{4, 29, 30}. Notably, the ionization energy IE^+ of the cation, i.e., the
164 *second* ionization energy of a neutral molecule, is higher than the *first* ionization energy IE^0 . This
165 is related to the on-site Coulomb interaction between electrons in the HOMO, commonly referred
166 to as Hubbard U ^{28, 31, 32}, which we directly determined here to be $U \approx 1.4$ eV (peak-to-peak split
167 between the occupied and unoccupied HOMO-derived sublevels of the cation obtained by UPS
168 and IPES, respectively) for a valence hole in solid C_{60} . Accordingly, the upper unoccupied
169 HOMO-derived sub-level of the cation is shifted by λ into the gap of the semiconductor and,
170 thereby, comes to lie above the HOMO of the neutral molecules in energy. The lower occupied
171 HOMO-derived sub-level appears at $U-\lambda$ outside the gap of the semiconductor, that is, below the
172 HOMO of the neutral molecules in energy. As shown in the center panel of Fig. 3(a), the energy
173 levels of neutral molecules residing in the Coulomb potential well ($\phi_{el,local}$) of the cation are
174 shifted by (up to) V , a quantity that can now, in analogy to U , be related to the inter-site Coulomb
175 interaction³³⁻³⁵.



178 Fig. 3 **Revised energy levels in molecular semiconductors comprising polarons:** (a) Origin of the
 179 experimentally observable spectral signature of cations from left to right: The reorganization
 180 energy λ corresponds to the difference between IE^0 and EA^+ . The on-site Coulomb-interaction U
 181 causes a splitting into two HOMO-derived sub-levels, EA^+ and IE^+ (with respect to a common
 182 vacuum level $\phi_{el,\infty}$), while inter-site Coulomb-interaction causes a distance dependent shift
 183 ($\phi_{el,loc}$) by up to V of the energy levels of the neutral molecules in close vicinity of the cations.
 184 The right-most panel shows a simplified projection, correcting the traditional view outlined in
 185 Fig.1 (b). (b) Analogous to (a) for negative polarons.
 186

187 Based on these observations, we provide a simplified picture of the single-particle energy levels
 188 associated with cations in an otherwise neutral molecular film in the rightmost panel of Fig. 3(a),
 189 which we suggest should replace the hitherto followed one in Fig. 1(c).

190 In full analogy, Fig. 3(b) revises the picture for molecules carrying a negative polaron^{2, 3, 10, 11}.
191 The energy gained from adding an electron onto a neutral molecule in the solid (EA^0) by IPES
192 equals the ionization energy of the relaxed anion (IE^-) minus the reorganization energy λ . The
193 electron affinity of the anion (EA^-), i.e., the *second* electron affinity of a neutral molecule, is now
194 lower than the *first* electron affinity EA^0 . This is again caused by the on-site Coulomb-interaction
195 between electrons in the LUMO. Therefore, the upper unoccupied LUMO-derived sub-level lies
196 at $U-\lambda$ outside the gap of the molecular semiconductor, and the lower occupied LUMO-derived
197 sub-level is found to be shifted by λ into the gap of the semiconductor. The energy levels of
198 neutral molecules within Coloumb-interaction range of nearby anions are shifted to lower binding
199 energy by (up to) an amount V , which depends again on the distance to the anion. The emerging
200 picture for the energy levels of anions in molecular solids, a simplified version of which is
201 provided in the rightmost panel of Fig. 3(b), implies that literature-based expectations^{10, 11} on
202 their spectral signature should be revised as well.

203

204 To summarize, we started out with the quest of obtaining the photoelectron spectral signature of
205 positively charged species in molecular semiconductors. To avoid potential masking of the
206 expected signal by parasitic effects, we relied on electron transfer from the molecular HOMO
207 across a thin, insulating interlayer to a metal substrate, thereby enabling the observation of "pure"
208 cations in the first place.

209 Supported by DFT calculations, we assessed the energy shift of the single-particle levels in
210 neutral molecules due to Coulomb-interaction with neighbouring cations to be $V \approx 0.5$ eV.
211 Naturally, the on-site Coulomb-interaction (Hubbard U) must exceed that value and was

212 determined here, in a complementary UPS/IPES study, to amount to $U \approx 1.4$ eV for the valence
213 hole in C_{60} . Most importantly, this term causes the ionization energy of cations to be substantially
214 higher than that of the respective neutral molecules, necessitating a fundamental revision of the
215 widely established picture of polarons in molecular semiconductors: Instead of finding a single,
216 singly occupied state within the gap of the neutral species, the respective frontier molecular
217 orbital level (i.e., the HOMO for positive and the LUMO for negative polarons) is split by on-site
218 Coulomb repulsion into an upper unoccupied sub-level and a lower occupied sub-level. For UPS
219 and IPES this implies that the spectral intensity associated with charged molecules does not
220 necessarily appear cut by E_F . Consequently, such molecular films are not metallic as long as U
221 dominates over weaker molecule-molecule and molecule-substrate interactions, which is often
222 the case in the bulk or on passivated substrates.

223 Our suggestion of replacing the widely established picture of polarons might lead to new insights
224 already from a re-interpretation of previous experimental results. More importantly, however, it
225 might inspire new experiments on the fundamental properties of charge carriers in weakly
226 interacting molecular systems, in particular, those induced by the electrical doping of molecular
227 semiconductors through admixing strong electron donors or acceptors.

228

229 **Acknowledgements**

230 This work was supported by the DFG (SPP1355, SFB951, and AM419/1-1) and the Helmholtz-
231 Energie-Allianz "Hybrid-Photovoltaik". We further acknowledge Stefan Krause for help with the
232 IPES-setup, Jürgen P. Rabe for providing access to the in-house multitechnique apparatus, Ruslan
233 Oysanikov and Oliver Monti for support at BESSY.

234 **Methods**

235 All samples were fabricated under ultra-high-vacuum conditions on an atomically clean Au(111)
236 single crystal (MaTecK, repeated Ar⁺-ion-sputtering and annealing cycles up to 550°C). MoO₃
237 (density = 4.7 g/cm³) and C₆₀ (density = 1.65 g/cm³) were purchased from Sigma Aldrich,
238 purified via re-sublimation prior to use, and deposited from resistively heated crucibles. The
239 evaporation rates (0.5-2 Å/min) and the nominal film thicknesses were monitored using a quartz-
240 crystal microbalance. The pressure during the evaporation did not exceed 5x10⁻⁸ mbar
241 (preparation chamber) and samples were transferred to the interconnected analysis chamber (base
242 pressure 3x10⁻¹⁰ mbar) without breaking the vacuum.

243 To assess the electronic structure across the Au/MoO₃/C₆₀-heterostructures, in-situ X-ray
244 photoelectron spectroscopy (XPS: photon energy $h\nu = 610$ eV) and UPS ($h\nu = 21$ eV) spectra
245 were collected at the end station SurICat (beamline PM4) of the synchrotron light source BESSY
246 II (Berlin, Germany) using a hemispherical electron-energy analyser Scienta SES 100. IPES was
247 performed in-house at HU-Berlin (incident electron energy range: 5-15 eV, NaCl-coated
248 photocathode, SrF₂-window).

249 Density-functional theory (DFT) calculations on isolated C₆₀ molecules were performed with a
250 hybrid exchange-correlation functional³⁶, mixing the generalized-gradient approximation
251 developed by Perdew, Burke and Ernzerhof³⁷ with a fraction α of Hartree-Fock (HF) exchange.
252 In the spirit of Refs.³⁸⁻⁴⁰, α was determined by imposing Janak's theorem⁴¹, that is, by requiring
253 that the total-energy difference between neutral and positively charged molecule (at the neutral-
254 molecule equilibrium structure) equals the eigenvalue of the highest occupied molecular orbital
255 of neutral C₆₀. To capture the screening of the excess hole on the fullerene by the environment
256 (MoO₃ and surrounding molecules), a polarizable continuum model⁴² with 3.5 as relative

257 dielectric constant was employed. After repeatedly cycling through the determination of α and the
258 geometry relaxation of the neutral molecule, an optimal value of $\alpha = 0.3147$ finally emerged. The
259 so-obtained hybrid-functional was then employed to relax the fullerene also to its (symmetry-
260 broken) cation equilibrium geometry. All calculations were performed with Gaussian 09, Rev.
261 A.02⁴³ using the triple- ζ polarized 6-311G** contracted-Gaussian basis set⁴⁴ for geometry
262 optimization and one set of additional diffuse functions (6-311+G**) for single-point
263 calculations⁴⁵.

264 The core-level density of states (DOS) was obtained by broadening the entire manifold of C1s-
265 related eigenvalues with area-normalized Gaussians of full-width at half-maximum (FWHM) of
266 0.7 eV. The valence DOS was produced by first broadening each valence-orbital eigenvalue with
267 an area normalized Gaussian of standard deviation $\sigma = 0.22$ eV to emulate disorder, by
268 subsequent multiplication with a room-temperature Fermi function (UPS) or one minus a Fermi
269 function (IPES), and by finally convoluting the result with an area-normalized Gaussian of $\sigma =$
270 0.14 eV (UPS) or $\sigma = 0.34$ eV (IPES) to account for detector broadening. For the spin-polarized
271 cations, possessing one more spin-up than spin-down electrons, two possible spin-multiplicities
272 (singlet and triplet) in the final state of the UPS/IPES experiment were taken into account:
273 Removing a further spin-down electron from the cation by UPS (or adding another spin-up
274 electron in IPES) results in one of three possible triplet states, while removing a spin-up electron
275 by UPS (or adding a spin-down electron in IPES) result in a singlet final state. Therefore, the
276 spin-down DOS for UPS (and the spin-up DOS in IPES) has been multiplied by a factor three
277 before adding the spin-up DOS for UPS (and the spin-down DOS for IPES) to yield the final
278 result displayed in Fig. 2 of the main text.

279

280 References

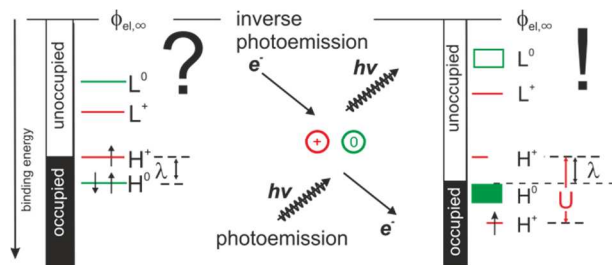
- 281 1. M. Pope and C. E. Swenberg, *Annu. Rev. Phys. Chem.*, 1984, **35**, 613-655.
- 282 2. J. L. Bredas and G. B. Street, *Acc. Chem. Res.*, 1985, **18**, 309-315.
- 283 3. S. Braun, W. R. Salaneck and M. Fahlman, *Adv. Mater.*, 2009, **21**, 1450-1472.
- 284 4. E. A. Silinsh, A. Klimkšans, S. Larsson and V. Čápek, *Chem. Phys.*, 1995, **198**, 311-331.
- 285 5. N. Karl, *Synth. Met.*, 2003, **133**, 649-657.
- 286 6. S. Kera, H. Yamane, I. Sakuragi, K. K. Okudaira and N. Ueno, *Chem. Phys. Lett.*, 2002, **364**, 93-98.
- 287 7. O. Bubnova, Z. U. Khan, H. Wang, S. Braun, D. R. Evans, M. Fabretto, P. Hojati-Talemi, D. Dagnelund, J. B. Arlin, Y. H. Geerts, S. Desbief, D. W. Breiby, J. W. Andreasen, R. Lazzaroni, W. M. M. Chen, I. Zozoulenko, M. Fahlman, P. J. Murphy, M. Berggren and X. Crispin, *Nature Mater.*, 2014, **13**, 190-194.
- 289 8. M. Fahlman, A. Crispin, X. Crispin, S. K. M. Henze, M. P. de Jong, W. Osikowicz, C. Tengstedt and W. R. Salaneck, *J. Phys.: Condens. Matter*, 2007, **19**, 183202.
- 291 9. W. Y. Gao and A. Kahn, *J. Appl. Phys.*, 2003, **94**, 359-366.
- 292 10. N. Koch, A. Rajagopal, J. Ghijsen, R. L. Johnson, G. Leising and J. J. Pireaux, *J. Phys. Chem. B*, 2000, **104**, 1434-1438.
- 293 11. D. Steinmuller, M. G. Ramsey and F. P. Netzer, *Phys. Rev. B*, 1993, **47**, 13323-13329.
- 294 12. M. Logdlund, R. Lazzaroni, S. Stafstrom, W. R. Salaneck and J. L. Bredas, *Phys. Rev. Lett.*, 1989, **63**, 1841-1844.
- 295 13. A. J. Heeger, *Polym J*, 1985, **17**, 201-208.
- 296 14. A. J. Heeger, S. Kivelson, J. R. Schrieffer and W. P. Su, *Rev. Mod. Phys.*, 1988, **60**, 781-850.
- 297 15. T. Sueyoshi, H. Fukagawa, M. Ono, S. Kera and N. Ueno, *Appl. Phys. Lett.*, 2009, **95**, 183303
- 298 16. I. Salzmann, G. Heimel, S. Duhm, M. Oehzelt, P. Pingel, B. M. George, A. Schnegg, K. Lips, R. P. Blum, A. Vollmer and N. Koch, *Phys. Rev. Lett.*, 2012, **108**, 035502.
- 300 17. H. Mendez, G. Heimel, A. Opitz, K. Sauer, P. Barkowski, M. Oehzelt, J. Soeda, T. Okamoto, J. Takeya, J. B. Arlin, J. Y. Balandier, Y. Geerts, N. Koch and I. Salzmann, *Angew. Chem., Int. Ed.*, 2013, **52**, 7751-7755.
- 301 18. G. Heimel, S. Duhm, I. Salzmann, A. Gerlach, A. Strozecka, J. Niederhausen, C. Bürker, T. Hosokai, I. Fernandez-Torrente, G. Schulze, S. Winkler, A. Wilke, R. Schlesinger, J. Frisch, B. Bröker, A. Vollmer, B. Detlefs, J. Pflaum, S. Kera, K. J. Franke, N. Ueno, J. I. Pascual, F. Schreiber and N. Koch, *Nature Chem.*, 2013, **5**, 187-194.
- 302 19. Y. Zou, L. Kilian, A. Scholl, T. Schmidt, R. Fink and E. Umbach, *Surf. Sci.*, 2006, **600**, 1240-1251.
- 303 20. S. L. Daifuku, C. Favaro, A. P. Marchetti and M. L. Neidig, *Org. Electron.*, 2014, **15**, 3761-3765.
- 304 21. C. D. Wagner, *Handbook of x-ray photoelectron spectroscopy: a reference book of standard data for use in x-ray photoelectron spectroscopy*, Physical Electronics Division, Perkin-Elmer Corp., 1979.
- 305 22. B. J. Topham, M. Kumar and Z. G. Soos, *Adv. Funct. Mater.*, 2011, **21**, 1931-1940.
- 306 23. P. Amsalem, J. Niederhausen, A. Wilke, G. Heimel, R. Schlesinger, S. Winkler, A. Vollmer, J. P. Rabe and N. Koch, *Phys. Rev. B*, 2013, **87**, 035440.
- 307 24. Irfan, M. L. Zhang, H. J. Ding, C. W. Tang and Y. L. Gao, *Org. Electron.*, 2011, **12**, 1588-1593.
- 308 25. H. B. Wang, P. Amsalem, G. Heimel, I. Salzmann, N. Koch and M. Oehzelt, *Adv. Mater.*, 2014, **26**, 925-930.
- 309 26. M. Oehzelt, N. Koch and G. Heimel, *Nat. Commun.*, 2014, **5**, 4174.
- 310 27. J. H. Weaver, *J. Phys. Chem. Solids*, 1992, **53**, 1433-1447.
- 311 28. R. Schwedhelm, L. Kipp, A. Dallmeyer and M. Skibowski, *Phys. Rev. B*, 1998, **58**, 13176-13180.
- 312 29. V. Coropceanu, J. Cornil, D. A. da Silva Filho, Y. Olivier, R. Silbey and J.-L. Brédas, *Chem. Rev.*, 2007, **107**, 926-952.
- 313 30. S. Kera, H. Yamane and N. Ueno, *Prog. Surf. Sci.*, 2009, **84**, 135-154.
- 314 31. J. Hubbard, *Proc. R. Soc. Lond. A*, 1963, **276**, 238-257.
- 315 32. B. Alvarez-Fernandez and J. A. Blanco, *Eur. J. Phys.*, 2002, **23**, 11-16.
- 316 33. E. Canadell, M.-L. Doublet and C. Iung, *Orbital Approach to the Electronic Structure of Solids*, Oxford University Press, 2012.
- 317 34. P. Hansmann, L. Vaugier, H. Jiang and S. Biermann, *J. Phys.: Condens. Matter*, 2013, **25**, 094005.
- 318 35. P. Fazekas, *Lecture notes on electron correlation and magnetism*, World Scientific, Singapore, River Edge, N.J., 1999.
- 319 36. C. Adamo and V. Barone, *J. Chem. Phys.*, 1999, **110**, 6158-6170.
- 320 37. J. P. Perdew, K. Burke and M. Ernzerhof, *Phys. Rev. Lett.*, 1996, **77**, 3865-3868.
- 321 38. T. Stein, H. Eisenberg, L. Kronik and R. Baer, *Phys. Rev. Lett.*, 2010, **105**, 266802.
- 322 39. S. Refaely-Abramson, R. Baer and L. Kronik, *Phys. Rev. B*, 2011, **84**, 075144.
- 323 40. V. Atalla, M. Yoon, F. Caruso, P. Rinke and M. Scheffler, *Phys. Rev. B*, 2013, **88**, 165122.
- 324 41. J. F. Janak, *Phys. Rev. B*, 1978, **18**, 7165-7168.
- 325 42. G. Scalmani and M. J. Frisch, *J. Chem. Phys.*, 2010, **132**, 114110.
- 326 43. G. W. T. M. J. Frisch, H. B. Schlegel, G. E. Scuseria, M. A. Robb, J. R. Cheeseman, G. Scalmani, V. Barone, B. Mennucci, G. A. Petersson, H. Nakatsuji, M. Caricato, X. Li, H. P. Hratchian, A. F. Izmaylov, J. Bloino, G. Zheng, J. L. Sonnenberg, M. Hada, M. Ehara, K. Toyota, R. Fukuda, J. Hasegawa, M. Ishida, T. Nakajima, Y. Honda, O. Kitao, H. Nakai, T. Vreven, J. A. Montgomery, Jr., J. E. Peralta, F. Ogliaro, M. Bearpark, J. J. Heyd, E. Brothers, K. N. Kudin, V. N. Staroverov, R.

- 337 Kobayashi, J. Normand, K. Raghavachari, A. Rendell, J. C. Burant, S. S. Iyengar, J. Tomasi, M. Cossi, N. Rega, J. M.
338 Millam, M. Klene, J. E. Knox, J. B. Cross, V. Bakken, C. Adamo, J. Jaramillo, R. Gomperts, R. E. Stratmann, O. Yazyev, A. J.
339 Austin, R. Cammi, C. Pomelli, J. W. Ochterski, R. L. Martin, K. Morokuma, V. G. Zakrzewski, G. A. Voth, P. Salvador, J. J.
340 Dannenberg, S. Dapprich, A. D. Daniels, O. Farkas, J. B. Foresman, J. V. Ortiz, J. Cioslowski, and D. J. Fox, ed. I. Gaussian,
341 Wallingford CT, Editon edn., 2009.
- 342 44. R. Krishnan, J. S. Binkley, R. Seeger and J. A. Pople, *J. Chem. Phys.*, 1980, **72**, 650-654.
- 343 45. M. J. Frisch, J. A. Pople and J. S. Binkley, *J. Chem. Phys.*, 1984, **80**, 3265-3269.

344

345

346



The widely established picture of polarons in molecular semiconductors is revised highlighting the role of on-site Coulomb repulsion.